



SIMULATION OF EARTHQUAKE MOTION AT NEAR FIELD REGION OF THE PAST DISASTROUS EARTHQUAKES

Masumitsu KUSE¹, Masata SUGITO² and Shinji KAWADE³

ABSTRACT

Simulation technique is presented to estimate strong ground motion especially at near field region of past disastrous earthquakes. For the estimation of strong ground motion at arbitrary sites in past earthquake, both the information on source parameters with sufficient accuracy and strong motion records obtained from the earthquake are incorporated into the techniques. In this study, two techniques are presented: One is the model to simulate the inherent spectral characteristics of the earthquake, and the other to simulate the effect of source process on the envelope of acceleration time histories. These techniques are based on the strong motion prediction model EMPR (Earthquake Motion Prediction model on Rock surface) developed by Sugito et al. (2000). These two specific information derived from seismic source are incorporated into the strong motion prediction model, EMPR. The availability of two techniques are examined regarding the ground motion intensity, spectral characteristic, and the envelope pattern of acceleration time histories.

Introduction

For the examination of the relations of the earthquake motion and the seismic damage, the reproduction of the earthquake motion is important. For the estimation of strong ground motion at arbitrary sites in past earthquake, both the information on source parameters with sufficient accuracy and strong motion records obtained from the earthquake are incorporated into the techniques.

In Niigata prefectures, Japan, two typical inland earthquakes occurred. One is The Mid Niigata Prefecture Earthquake in 2004 (M=6.8), and the other is The Niigataken Chuetsu-oki Earthquake in 2007 (M=6.8). In these earthquakes, many strong motion records were obtained by K-NET and KiK-net (2009), which are the observation network operated by National Research Institute for Earth Science and Disaster Prevention.

In this study, the source parameters are examined from two techniques, and the strong motion is estimated. More specifically, we used for estimation of (1) the general spectral characteristic, and (2) the source process of this earthquake. These two specific information

¹ Assistant Professor, River Basin Research Center, Gifu University, Gifu City, Japan

² Professor, River Basin Research Center, Gifu University, Gifu City, Japan

³ Gifu Prefectural Government, Gifu City, Japan

derived from seismic source are incorporated into the strong motion prediction model, EMPR (Sugito, et al., 2000). In the following, these two techniques used for this study are outlined, and its application to estimation of the source parameters in these earthquakes, are presented.

Simulation Technique of strong ground motion for Past Disastrous Earthquake Outline of Earthquake Motion Prediction Model on Rock Surface [EMPR]

Nonstationary strong motion prediction model, EMPR, was developed of Sugito et al.(2000). EMPR was developed on the basis of rock surface strong motion dataset. The strong motion dataset consists of 118 components of major Japanese accelerograms including the records from the 1995 Hyogoken-nanbu Earthquake.

Earthquake acceleration with nonstationary frequency content can be represented by Eq. 1.

$$x(t) = \sum_{k=1}^m \sqrt{4\pi \cdot G_x(t, 2\pi f_k)} \cdot \Delta f \cdot \cos(2\pi f_k t + \phi_k) \quad (1)$$

in which $\sqrt{G_x(t, 2\pi f_k)}$ is evolutionary power spectrum (Kameda, 1975) for time t and frequency f_k , ϕ_k is independent random phase angles distributed over $0 \sim 2\pi$, and m is the number of superposed harmonic components.

The upper and lower boundary frequencies, f_u, f_l , are fixed as $f_u = 10.03$ (Hz), and also m and Δf are fixed as $m=166$ and $\Delta f = 0.06$ (Hz). The following time-varying function is adopted for the model of $\sqrt{G_x(t, 2\pi f_k)}$.

$$\sqrt{G_x(t, 2\pi f)} = \alpha_m(f) \frac{t - t_s(f)}{t_p(f)} \exp\left\{1 - \frac{t - t_s(f)}{t_p(f)}\right\} \quad (2)$$

in which $t_s(f)$, $t_p(f)$ are starting time and duration parameter, respectively, and α_m is intensity parameter which represents the peak value of $\sqrt{G_x(t, 2\pi f_k)}$. These parameters have been determined relative to recorded acceleration time histories. Fig. 1 shows example of recorded and modeled evolutionary spectra.

In addition, as shown Fig. 2, the evolutionary spectra for great earthquake is incorporated the effect of fault size, successive fault rupture, and rupture direction, on characteristics of ground motion.

The superposed evolutionary spectra for great earthquake is given by Eq. 3.

$$\sqrt{G_x(t, 2\pi f_k)} = \frac{\beta(f, M_0) \cdot N_G(M_0)}{N_x \cdot N_y} \sum_{i=1}^{N_x} \sum_{j=1}^{N_y} \sqrt{G_{ij}(t, 2\pi f_k)} \quad (3)$$

where G_{ij} is evolutionary spectrum for each unit event corresponding to the earthquake magnitude $M=6.0$ and hypo-central distance R_{ij} , and the suffix, i and j , represent the position of each event on the fault. N_x and N_y represent the number of unit event in the direction of fault width and length. The number of superposition, $N_G(M_0)$ is the average of the magnification factor that is calculated the range from 0.13(Hz) to 10.03(Hz). $\beta(f, M_0)$ is the correction factor.

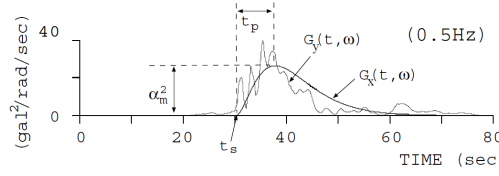


Figure 1. Recorded and simulated evolutionary power spectra.

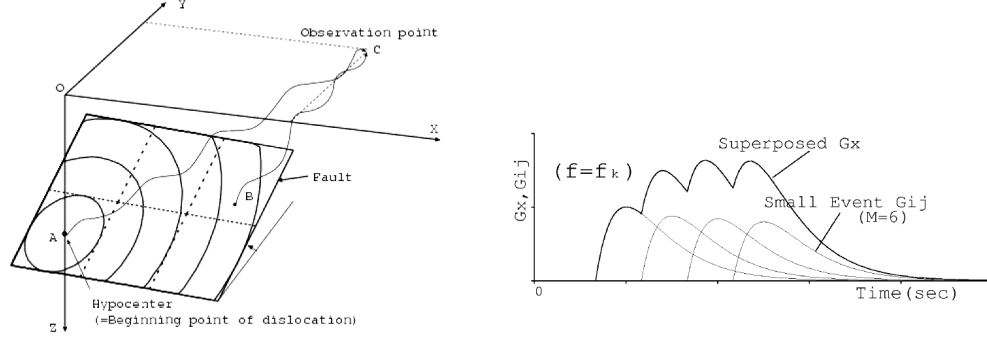


Figure 2. Fault modeling with multiple fault rupture and superposed evolutionary power spectra.

Simulation Technique for Past Disastrous Earthquake

In this study, two techniques are presented. One is the model to simulate the inherent spectral characteristic of the earthquake, and the other to simulate the effect of source process on the envelope of acceleration time histories. Fig. 3 shows the concept of the simulation techniques. As shown in this figure, the spectral characteristics is incorporated clearly in the response spectrum (EMPR-S), and the effect of the source process is incorporated in the envelope of acceleration time history (EMPR-A).

Technique for correction of spectral characteristic [EMPR-S]

The spectral characteristic common in all over the near-source area is obtained from the recorded acceleration time histories, and they are incorporated into the simulation technique.

In the basic simulation model, EMPR, the number of superposition of evolutionary spectrum corresponding to the earthquake of $M=6.0$ is given by $\beta(f, M_0) \times N_G(M_0)$. As shown Eq. 4, Furumoto et al.(2008) showed the general spectral characteristic that was used $A_p(f)$ on instead $\beta(f, M_0) \times N_G(M_0)$.

$$A_p(f) = \frac{\alpha'_m(f) \cdot t'_p(f)}{\bar{\alpha}_m(f) \cdot \bar{t}_p(f)} \quad (4)$$

where, $\bar{\alpha}_m(f)$, $\bar{t}_p(f)$ are given from the EMPR which corresponds to the earthquake magnitude $M=6.0$ and the same hypo-central distance of the specific data. $\alpha'_m(f)$, $t'_p(f)$ are given from the free rock surface wave motion corresponds to the observed record.

Technique for inversion of source process [EMPR-A]

Fig. 4 shows the flow of the inversion method by Kuse et al.(2004a). In the analysis, the

location of hypocenter (latitude, longitude, depth) and the fault parameters (length, width, strike, dip angle) are dealt with as the given parameters. The inversion method consists of two steps: STEP 1 for estimation of the seismic moment and the propagation velocity of fault rupture and STEP 2 for inversion of asperity pattern. In STEP 1, the seismic moment, M_0 , and the propagation velocity of rupture, v_r , are identified. The details are described in Kuse et al.(2000). At this stage the asperity distribution on the fault plane is not considered. The two ground motion parameters are used for the inversion of M_0 and v_r ; one is the acceleration total power, P_t , and the other, the strong motion duration, t_{90} . The acceleration total power, P_t , defined by Eq. 5 represents the square sum of acceleration time history over the total record length T :

$$P_t = \int_0^T \{x(t)\}^2 dt \quad (5)$$

where, P_t is the acceleration total power (cm^2/sec^3), $x(t)$ is the acceleration (cm/sec^2) at time t , T is the total record length of the accelerogram (sec). The parameter, t_{90} , represents the duration defined as the time length between 5% and 95 % in terms of the accumulation of acceleration power.

Next, in the STEP 2, the inversion of normalized ratio of released acceleration power on the fault plane is performed using the seismic moment, M_0 , and the propagation velocity of rupture, v_r , obtained in STEP1. Kuse et al.(2004a, 2004b) proposed two alternative ways of processing acceleration time histories; one deals with the envelope of acceleration time history, and the other deals with the envelope of bandpass-filtered acceleration time history for low, middle, and high frequency ranges. In this paper, the envelope of acceleration time history for the estimation of asperity pattern was employed.

Application to the Recent Earthquakes

Fault Parameters and Strong Motion Dataset

Outline of two earthquakes and strong motion records

These techniques presented above are applied to the Mid Niigata Prefecture Earthquake in 2004, and the Niigataken Chuetsu-oki Earthquake in 2007. Fig. 5 shows locations of the fault and the strong motion stations of KiK-net(2009) around focal region. These records used in the analysis were obtained at the stations represented by circled numbers in Fig.5. The projection of the fault plane on the ground surface is also given in Fig. 5. As shown Table 1, the horizontal components of acceleration records obtained these stations were used in the analysis. These records were converted to those on rock surface level with the shear wave velocity of 500(m/sec).

Table 2 shows the fault parameters of these two earthquakes, including the estimated parameters, M_0 and v_r , which were obtained through the inversion process at STEP1 in Fig. 4.

Dataset of strong ground motion on rock surface

In this study, the dataset of strong motion records that were observed by KiK-net (2009) stations, were used. Generally two seismometer both on ground surface and underground base rock level are set in the KiK-net system. These techniques for estimation of source parameter used here is based on the strong motion prediction model, EMPR (Sugito et al., 2000). The EMPR that was used for the analysis is the strong motion prediction model on the rock surface

that was defined as the shear wave velocity of 400-600(m/sec). Therefore, as shown Fig. 4, these records were converted to those on the rock surface level with the shear wave velocity of approximately 400-600(m/sec).

Fig. 6 shows the outline of conversion for the strong motion records. First, the record on rock surface level (over 500(m/sec)) was converted based on the soil profile models for these observation stations. The response analysis of layered ground, using the program code FDEL (Frequency Dependent Equi-Linearized technique) (Sugito et al., 1995), has been applied. In this analysis, the lower limits of damping h_{min} for the rock and harder layer (over 500(m/sec)) was fixed as $h_{min}=2\%$ based on Enomoto et al.(2007). In case of other soils (clay, silt, sand, gravel), the lower limit was fixed as $h_{min}=5\%$.

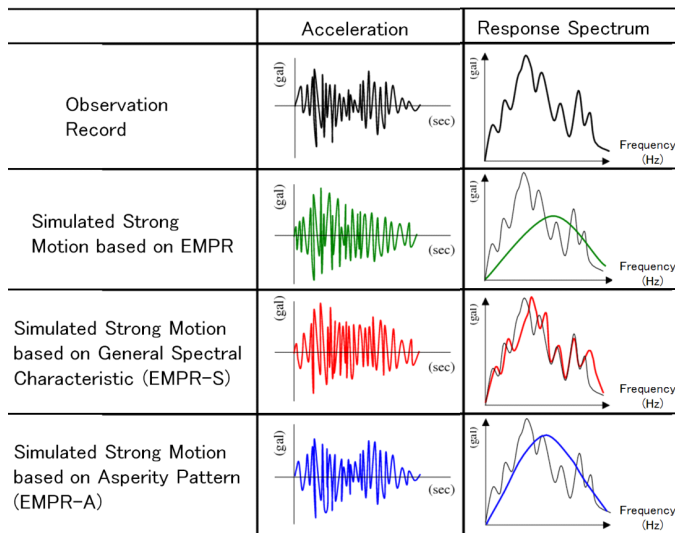


Figure 3. Concept of simulation technique compared with original EMPR model.

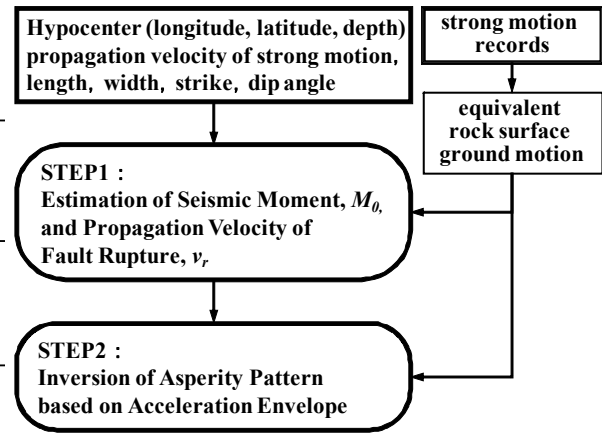


Figure 4. Outline for inversion of source process.

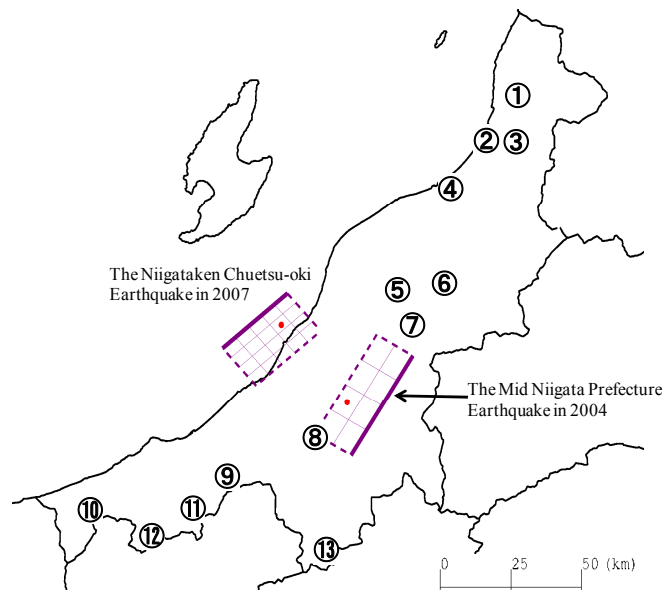


Figure 5. Location of strong motion stations and faults (Red circle represents epicenter, circled number represents location of observation stations).

Table 1. List of strong motion records.

(a) The Mid Niigata Prefecture Earthquake in 2004.

(b) The Niigataken Chuetsu-oki Earthquake in 2007.

| No. | Station Code | Maximum Acceleration on Soil Surface (cm/sec ²) | | Maximum Acceleration on Rock Surface (Vs=500m/sec) (cm/sec ²) | | Epicentral Distance (km) |
|-----|--------------|---|---------|---|---------|--------------------------|
| | | EW | NS | EW | NS | |
| | | ① | NIGH02 | -30.51 | -40.2 | |
| ② | NIGH03 | -25.67 | 31.81 | -12.82 | 12.51 | 107.7 |
| ③ | NIGH04 | 56.59 | 47.59 | 28.25 | -19.41 | 113.1 |
| ④ | NIGH05 | -91.1 | 92.38 | 26.50 | 27.60 | 86.0 |
| ⑤ | NIGH06 | 407.22 | 364.43 | 240.39 | 160.45 | 45.6 |
| ⑥ | NIGH07 | -97.35 | -96.52 | 55.61 | -61.00 | 57.5 |
| ⑦ | NIGH09 | -375.39 | 394.32 | -138.27 | 220.68 | 39.3 |
| ⑧ | NIGH11 | -576.67 | -462.92 | -358.69 | -353.35 | 15.2 |
| ⑨ | NIGH13 | 85.91 | 68.08 | -52.80 | 32.34 | 45.0 |
| ⑩ | NIGH16 | 29.21 | 26.77 | 23.22 | 14.43 | 93.4 |
| ⑪ | NIGH18 | -111.47 | -95.96 | 40.76 | 51.91 | 62.3 |

| No. | Station Code | Maximum Acceleration on Soil Surface (cm/sec ²) | | Maximum Acceleration on Rock Surface (Vs=500m/sec) (cm/sec ²) | | Epicentral Distance (km) |
|-----|--------------|---|---------|---|---------|--------------------------|
| | | EW | NS | EW | NS | |
| | | ① | NIGH02 | 48.38 | 26.23 | |
| ② | NIGH03 | -23.99 | 28.15 | -9.13 | 14.94 | 96.4 |
| ③ | NIGH04 | -59.67 | -60.65 | -26.70 | 32.44 | 104.0 |
| ④ | NIGH05 | -69.26 | 75.47 | -24.55 | 26.54 | 75.1 |
| ⑤ | NIGH06 | -148.38 | -149.2 | -51.75 | -57.20 | 41.8 |
| ⑥ | NIGH07 | -66.59 | -72.38 | 29.28 | 24.90 | 58.8 |
| ⑦ | NIGH09 | -123.47 | 121.83 | 46.86 | -67.19 | 45.9 |
| ⑧ | NIGH11 | 124.11 | 161.31 | 70.75 | 103.30 | 44.4 |
| ⑨ | NIGH13 | -165.9 | 261.25 | 120.76 | -126.23 | 58.9 |
| ⑩ | NIGH16 | 72.78 | 49.01 | -67.89 | 32.45 | 96.3 |
| ⑪ | NIGH18 | -95.87 | -94.96 | -68.44 | 51.72 | 75.0 |
| ⑫ | NIGH17 | -17.89 | -25.51 | -20.40 | -17.71 | 90.1 |
| ⑬ | NIGH19 | -47.57 | -131.13 | -14.96 | -27.36 | 84.4 |

Table 2. Fault parameters.

| Fault Parameter | | The Mid Niigata Prefecture Earthquake in 2004 | The Niigataken Chuetsu-oki Earthquake in 2007 |
|--|-------------------|---|---|
| Hypocenter | Latitude(degree) | 37.29 | 37.54 |
| | Longitude(degree) | 138.87 | 138.61 |
| | Depth(km) | 13.4 | 8.0 |
| Fault Plane (after Honda et al., 2004, Aoi et al., 2007) | Length(km) | 42.0 | 30.0 |
| | Width(km) | 24.0 | 24.0 |
| | Strike(degree) | 211.0 | 49.0 |
| | Dip Angle(degree) | 52.0 | 42.0 |
| *Seismic Moment M_0 (Nm) | | 2.46×10^{18} | 1.83×10^{18} |
| *Propagation Velocity of Fault Rupture v_r (km/sec) | | 1.89 | 1.89 |

(Estimated in STEP1 at Fig.4)

Next, the free-rock surface ground motions were converted to those for the shear wave velocity of 500(m/sec) based on Midorikawa (1987). The amplification of earthquake motion from the seismic bedrock ($V_s=3,000$ (m/sec)) to the surface is represented in the following equation.

$$A_v = \begin{cases} 170v_s'^{-0.6} & (v_s' < 1100 \text{ (m/sec)}) \\ 2.5 & (v_s' \geq 1100 \text{ (m/sec)}) \end{cases} \quad (6)$$

where, A_v is the amplitude ratio of maximum velocity from the seismic bedrock to the surface, V_s' is the average of shear wave velocity at 30(m) below the surface of ground (m/sec). The correction factor, A , of acceleration time history from rock surface level of $V_s=V_{sx}$ to $V_s=500$ (m/sec) is given in the following.

$$A = \left(\frac{500}{v_{sx}} \right)^{-0.6} \quad (7)$$

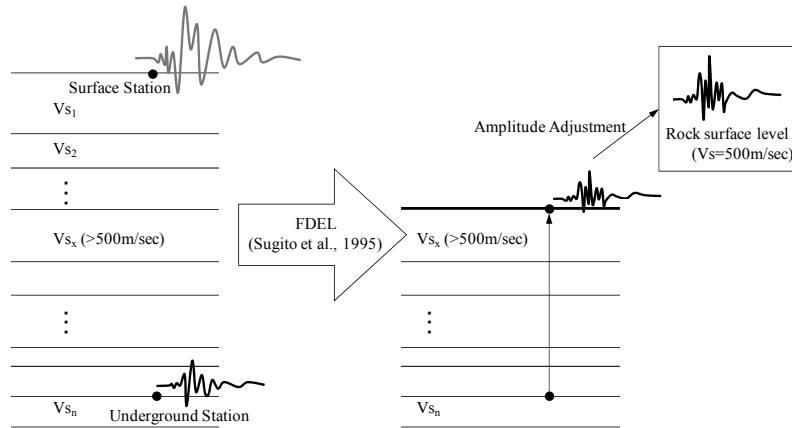


Figure 6. Schematic diagram for calculation of rock surface ground motion with shear wave velocity of $V_s=500(\text{m/sec})$.

where, A is the correction factor of the earthquake motion, V_{sx} is the shear wave velocity on the rock surface at each individual KiK-net site (See Fig. 6).

Simulation of Strong Ground Motion

Correction of spectral characteristic [EMPR-S]

Fig. 7 shows the number of superposition of evolutionary power spectra. The green lines in Fig. 7 represent the number of superposition obtained from corrected strong motion records at many observation stations. The variability of record is effect that the number of superposition is included both the source property and the propagation characteristic.

As shown Fig. 7, the number of superposition as the general spectral characteristic can compare the peculiar characteristic of every earthquake. The low frequency range of both earthquakes is relatively large. At the range around 1(Hz), the Niigataken Chuetsu –oki Earthquake in 2007 is larger than the Mid Niigata Prefecture Earthquake in 2004.

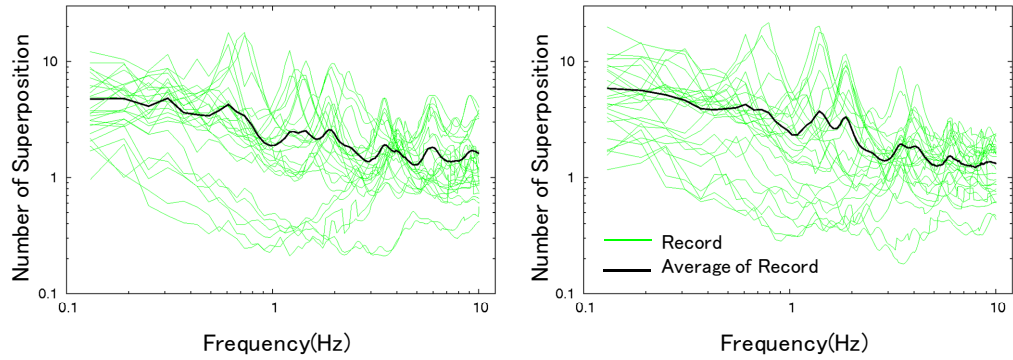
Inversion of source process [EMPR-A]

The inversion method presented above was applied. As previously mentioned, these records were converted to those on rock surface level with the shear wave velocity of 500(m/sec).

Figs. 8, 9 shows the asperity pattern that has been obtained the STEP 2 at Fig. 4. For comparison, Fig. 8(a) and Fig. 9(b) shows the distribution of coseismic slip estimated by Honda et al.(2004) and Aoi et al.(2007). The location of asperity for these analysis are consistent.

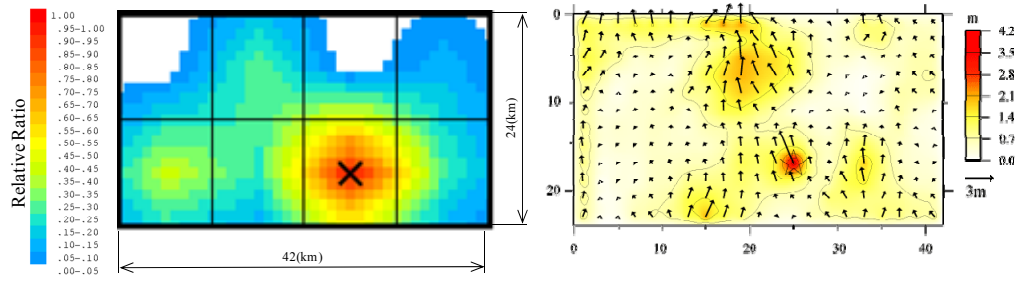
Comparison of simulated and recorded strong motion

These two information derived from seismic source can incorporate into the strong motion prediction model, EMPR. Fig. 10 shows the comparison of acceleration time histories and fourier spectrum at NIGH09. The recorded acceleration time histories at Fig. 10 (a), (e), are converted to rock surface level with the shear wave velocity of 500(m/sec). As shown Fig. 10, the simulated acceleration time history and the fourier spectrum based on estimated source parameter are improved.



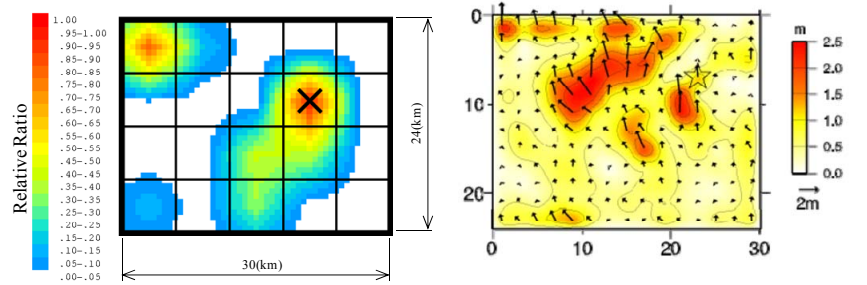
(a) The Mid Niigata Prefecture Earthquake in 2004. (b) The Niigataken Chuetsu-oki Earthquake in 2007.

Figure 7. Number of superposition of evolutionary spectra obtained from strong motion Records.



(a) Asperity pattern (This study). (b) Distribution of fault slip (Honda et al., 2004).

Figure 8. Distribution of asperity (The Mid Niigata Prefecture Earthquake in 2004).



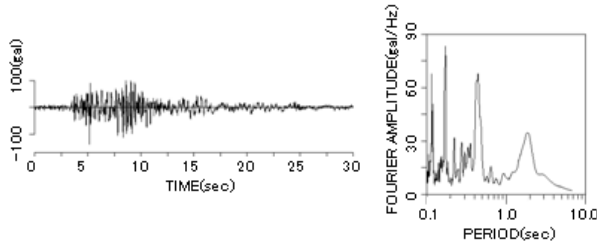
(a) Asperity pattern (This study). (b) Distribution of fault slip (Aoi et al., 2007).

Figure 9. Distribution of asperity (The Niigataken Chuetsu-oki Earthquake in 2007).

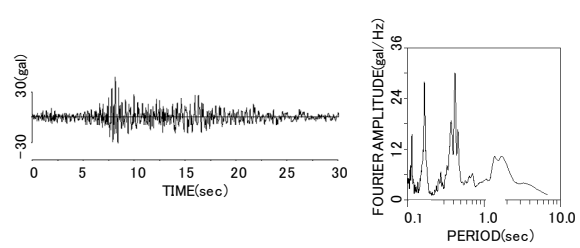
Conclusions

The simulation technique was presented to estimate strong ground motion especially at near field region of past disastrous earthquakes. The major results derived here may be summarized as follows.

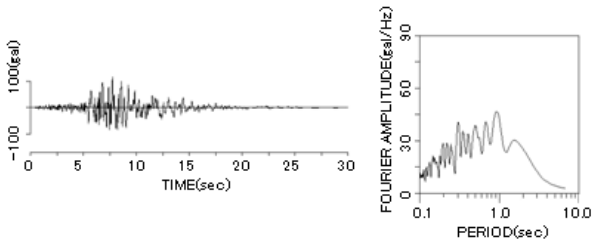
1. The dataset of strong motion records on rock surface for recent two earthquakes were arranged for the application of the simulation technique developed by the authors. The original records were obtained at underground bed rock level in KiK-net observation systems during the Mid Niigata Prefecture Earthquake in 2004 and the Niigataken Chuetsu-oki Earthquake in 2007.



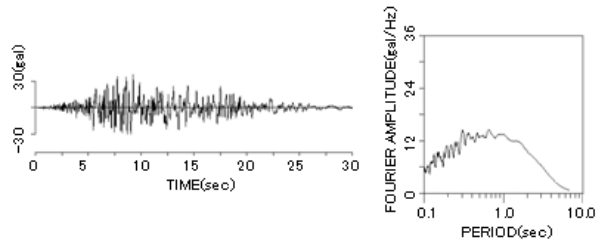
(a) The Mid Niigata Prefecture Earthquake in 2004 (Recorded).



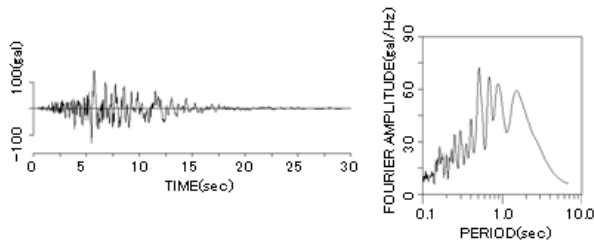
(e) The Niigataken Chuetsu-oki Earthquake in 2007 (Recorded).



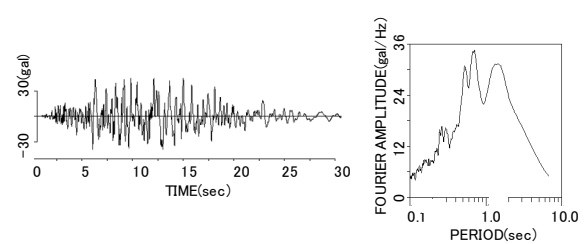
(b) The Mid Niigata Prefecture Earthquake in 2004 (Simulated by EMPR).



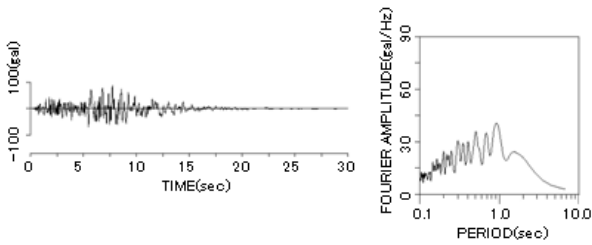
(f) The Niigataken Chuetsu-oki Earthquake in 2007 (Simulated by EMPR).



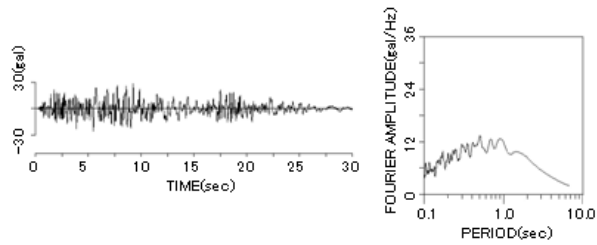
(c) The Mid Niigata Prefecture Earthquake in 2004 (Simulated by EMPR-S).



(g) The Niigataken Chuetsu-oki Earthquake in 2007 (Simulated by EMPR-S).



(d) The Mid Niigata Prefecture Earthquake in 2004 (Simulated by EMPR-A).



(h) The Niigataken Chuetsu-oki Earthquake in 2007 (Simulated by EMPR-A).

Figure 10. Comparison of acceleration time histories and fourier spectrum (NIGH09, EW).

2. The general spectral characteristic, which was named the number of superposition of evolutionary spectra were estimated by Furumoto et al(2008). The ratio of power from several typical earthquake records obtained recently in Japan and that from statistical mean value of past earthquake records which is equivalent to $M=6$ is derived every frequency in the range of $0.1\sim 10.0\text{Hz}$, and the characteristics of each earthquake motion are considered. We estimate the ration of power from target earthquake obtained by the strong motion records.
3. The asperity distributions were estimated by inversion technique developed by the authors. In the analysis, the acceleration envelope for the unit sub-event motion given by the strong

motion prediction model, EMPR, was applied. The asperity pattern obtained in this study represents the relative ratio of release of acceleration power over the fault.

4. Case studies of the earthquake simulation by the presented techniques were performed. The simulated rock surface motions were compared with observed motions in terms of the acceleration time history and fourier spectrum. The applicability of the two simulation techniques were demonstrated.

Acknowledgments

The authors would like to express their deep appreciation to Dr, Yoshinori Furumoto of Nagano National College of Technology for support of numerical calculation for the general spectral characteristic. In this paper, the strong motion recorded from KiK-net system was used in this study.

References

- Aoi, S., Sekiguchi, H., Morikawa, N., Kunugi, K., and Shirasaka, M, 2007. Source Process of the 2007 Niigata-ken Chuetsu-oki Earthquake Derived from Near-fault Strong Motion Data. http://www.k-net.bosai.go.jp/k-net/topics/chuetsuoki20070716/inversion/ksw_ver070816_NIED_Inv_eng.pdf.
- Enomoto, Y., Sugito, M., and Kuse, M., 2007. The Study of Earthquake Response Analysis based on the KiK-net Records. *JSCE-Chubu Annual Meeting*, I-20 (in Japanese)
- Furumoto, Y., Kuse, M., Kawade, S., and Sugito, M, 2008. Simulation of Non-Stationary Strong Ground Motions During Past Earthquakes Based on the Fault Parameters and the Spectral Characteristics of Recorded Accelerogram, *14th World Conference on Earthquake Engineering*, Paper No.07-0182.
- Honda, R., Aoi, S., Sekiguchi, H., Morikawa, N., Kunugi, T., and Fujiwara, H, 2004. Ground Motion and Rupture Process of the 2004 Mid Niigata Prefecture Earthquake Obtained from Strong Motion Data of K-NET and KiK-net, http://wwwold.k-net.bosai.go.jp/k-net/topics/niigata041023/index_e.html
- Kameda, H, 1975. Evolutionary Spectra of Seismogram by Multifilter, *Journal of Engineering Mechanics Division*, ASCE, Vol.101, 787-801.
- K-NET and KiK-net, 2009. Strong-motion Seismograph Networks Portal Site, National Research Institute for Earth Science and Disaster Prevention, http://www.kyoshin.bosai.go.jp/index_en.html
- Kuse, M., Sugito, M., and Nojima, N, 2004b. Inversion of Source Process in Consideration of Filtered-Acceleration Envelope, *13th World Conference on Earthquake Engineering*, Paper No.665.
- Kuse, M., Sugito, M., Nojima, N., and Yagyuu, K, 2004b. Inversion of Source Process in Consideration of Filtered-Acceleration Power Time Histories. *Journal of Structural Mechanics and Earthquake Engineering* I-67: No, 759, 409-414. (in Japanese)
- Midorikawa, S, 1987. Prediction of Iseismic Map in the Kanto Plain due to Hypothetical Earthquake, *Journal of Structural Engineering*, Vol.33B, 43-48. (in Japanese)
- Sugito, M, 1995. Frequency-dependent Equivalent Strain for Earthquake Response Analysis of soft Ground, *Proc. of IS-Tokyo, '95, The First International Conference on Earthquake Geotechnical Engineering*, 655-660.
- Sugito, M., Furumoto, Y., and Sugiyama, T, 2000. Strong Motion Prediction on Rock Surface by Superposed Evolutionary Spectra. *12th World Conference on Earthquake Engineering*, Paper No.2111.